Green's functions for the two-dimensional radiative transfer equation in bounded media

2012 J. Phys. A: Math. Theor. 45 175201

(http://iopscience.iop.org/1751-8121/45/17/175201)

IOP Publishing Journal of Physics A: Mathematical and Theoretical

J. Phys. A: Math. Theor. **45** (2012) 175201 (9pp) doi:10.1088/1751-8113/45/17/175201

Green's functions for the two-dimensional radiative transfer equation in bounded media

André Liemert and Alwin Kienle

Institut für Lasertechnologien in der Medizin und Meßtechnik, Helmholtzstr.12, D-89081 Ulm, Germany

E-mail: alwin.kienle@ilm.uni-ulm.de

Received 14 November 2011, in final form 9 March 2012
Published 11 April 2012
Online at stacks.iop.org/JPhysA/45/175201

Abstract

In this study, the two-dimensional radiative transfer equation is solved considering the exact boundary conditions for describing the propagation of particles in bounded anisotropically scattering media. The obtained Green's functions have an analytical dependence on the spatial and angular variables and, therefore, can be evaluated rapidly and implemented without any computational complexities. The Monte Carlo method was used for a successful verification of the derived solutions.

PACS numbers: 05.60.Cd, 42.68.Ay, 95.30.Jx

(Some figures may appear in colour only in the online journal)

1. Introduction

The radiative transfer equation (RTE) is involved in many areas of physics to describe diverse transport processes [1–3]. The mathematical complexity of this integro-partial differential equation implies that solutions which are used for studying the propagation of waves and particles in anisotropically scattering media bounded by a curved or planar contour are mostly based on numerical approaches such as the Monte Carlo method [4], the discrete-ordinate method [5] or the finite-difference method [6]. The main disadvantages of the numerical methods compared to the available analytical solutions are the long computational times and the complexities regarding the numerical implementation. However, in cases when the scattering medium is bounded by an arbitrary complex contour, the corresponding solutions to the RTE are in general based completely on numerical methods. The authors of [7–9] developed elegant analytical approaches regarding the three-dimensional RTE for obtaining Green's function for the infinite medium and in media with planar boundaries such as the slab geometry, resulting in a much smaller computational cost than is needed with the conventional spherical harmonics method. Alternatively, Kim *et al* [10, 11] derived solutions of the three-dimensional RTE using

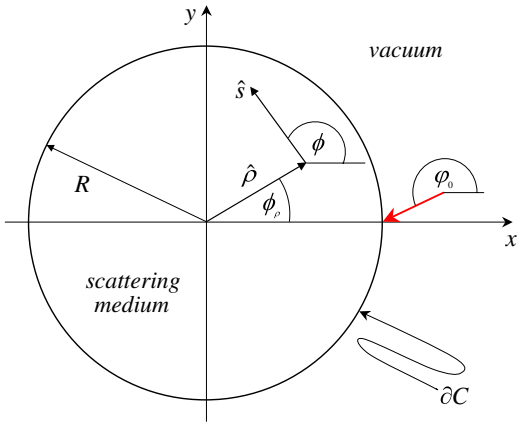

Figure 1. Circular bounded medium with spatial and angular variables.

a plane-wave decomposition of the radiance and by solving the resulting eigenvalue problem numerically via discretization of the angular variables.

In some cases, the two-dimensional RTE is used as an appropriate radiative transfer model [5, 12–14]. Recently, we derived the infinite space Green's function of the two-dimensional RTE [15] in the steady state and time domains. In this paper, we generalized our previous solution to the more important case of bounded media, i.e. for a circular and a semi-infinite geometry, by considering the exact boundary conditions (BC). Similar to those of the unbounded medium, the resulting Green's functions are apart from several eigenvalues and the solution of linear equations analytically regarding the spatial and angular variables. The derived expressions were successfully verified by comparisons with our Monte Carlo code [16].

2. Theory

2.1. Radiative transfer in a circular region

The two-dimensional homogeneous RTE for the radiance $\psi(\boldsymbol{\rho}, \phi)$ in Cartesian coordinates is given by

$$\hat{\mathbf{s}} \cdot \nabla \psi(\boldsymbol{\rho}, \phi) + \mu_t \psi(\boldsymbol{\rho}, \phi) = \mu_s \int_0^{2\pi} f(\hat{\mathbf{s}} \cdot \hat{\mathbf{s}}') \psi(\boldsymbol{\rho}, \phi') \, \mathrm{d}\phi', \tag{1}$$

where $\mu_t = \mu_a + \mu_s$ is the total attenuation coefficient, μ_a is the absorption coefficient and μ_s is the scattering coefficient. The angle ϕ describes the direction of the propagation vector $\hat{\mathbf{s}}$. The phase function $f(\hat{\mathbf{s}} \cdot \hat{\mathbf{s}}')$ describes the probability that a particle coming from the direction $\hat{\mathbf{s}}'$ is scattered in the direction $\hat{\mathbf{s}}$.

For obtaining the solution of the boundary-value problem in a circular bounded region, it is advantageous to use the radiance in polar coordinates leading to $\psi = \psi(\rho, \phi_{\boldsymbol{\rho}}, \varphi)$, where $\varphi = \phi - \phi_{\boldsymbol{\rho}}$. Here, it is assumed that a narrow incident beam having an arbitrarily direction φ_0 enters the circular region from the vacuum at the boundary $\partial\mathcal{C}$. For illustration, figure 1 shows schematically the geometry of the problem including all spatial and angular variables

used within the derivations. The evaluation of the corresponding total differentials leads to the RTE in polar coordinates:

$$\cos\varphi\frac{\partial\psi}{\partial\rho}+\frac{\sin\varphi}{\rho}\left(\frac{\partial\psi}{\partial\phi_\rho}-\frac{\partial\psi}{\partial\varphi}\right)+\mu_t\psi=\mu_s\int_0^{2\pi}f(\hat{\mathbf{s}}\cdot\hat{\mathbf{s}}')\psi(\boldsymbol{\rho},\varphi')\,\mathrm{d}\phi'. \tag{2}$$

The solution of the boundary-value problem in the circular geometry involves the inhomogeneous BC:

$$\psi(\boldsymbol{\rho}\in\partial\mathcal{C},\varphi)=S_0\delta(\phi_{\boldsymbol{\rho}})\delta(\varphi-\varphi_0),\qquad\hat{\mathbf{s}}\cdot\hat{\boldsymbol{\rho}}<0, \tag{3}$$

where $\partial\mathcal{C}$ denotes the contour of the circular region and S_0 is a constant. The radiance is a 2π-periodic function and therefore can be written as

$$\psi(\boldsymbol{\rho},\varphi)=\sum_{n=-\infty}^{\infty}\psi_n(\rho,\varphi)\exp(\mathrm{i}n\phi_{\boldsymbol{\rho}}). \tag{4}$$

Inserting this series in the RTE (2) results in the following equation for the functions $\psi_n=\psi_n(\rho,\varphi)$:

$$\cos\varphi\frac{\partial\psi_n}{\partial\rho}+\frac{\sin\varphi}{\rho}\left(\mathrm{i}n\psi_n-\frac{\partial\psi_n}{\partial\varphi}\right)+\mu_t\psi_n=\mu_s\int_0^{2\pi}f(\hat{\mathbf{s}}\cdot\hat{\mathbf{s}}')\psi_n(\rho,\varphi')\,\mathrm{d}\phi'. \tag{5}$$

The BC which must be satisfied by the expansion coefficients becomes

$$\psi_n(\rho=R,\varphi)=\frac{S_0}{2\pi}\delta(\varphi-\varphi_0),\qquad\pi/2\leqslant\varphi\leqslant3\pi/2. \tag{6}$$

For solving equation (5), we seek a solution in the form of the following mode:

$$\psi_n(\rho,\varphi)=\sum_{m=-\infty}^{\infty}(-1)^m\langle m|u_n\rangle I_{m-n}\left(\frac{\rho}{\lambda}\right)\mathrm{e}^{\mathrm{i}m\varphi}, \tag{7}$$

where $I_\nu(x)$ denotes the modified Bessel function of the first kind and $|u_n\rangle$ are unknown vectors with components $\langle m|u_n\rangle$. The substitution of this mode in (5) yields the eigenvalue problem

$$\langle m-1|u_n\rangle+\langle m+1|u_n\rangle-2\lambda\sigma_m\langle m|u_n\rangle=0, \tag{8}$$

where $\sigma_m=\mu_a+(1-f_m)\mu_s$. Note that for obtaining the above characteristic equation the phase function is also used in the form

$$f(\hat{\mathbf{s}}\cdot\hat{\mathbf{s}}')=\frac{1}{2\pi}\sum_{m=-\infty}^{\infty}f_m\mathrm{e}^{\mathrm{i}m(\phi-\phi')}, \tag{9}$$

with the corresponding coefficients

$$f_m=\int_0^{2\pi}f(\hat{\mathbf{s}}\cdot\hat{\mathbf{s}}')\,\mathrm{e}^{-\mathrm{i}m(\phi-\phi')}\,\mathrm{d}\phi'. \tag{10}$$

For the Henyey–Greenstein model in two dimensions, the resulting expansion coefficients are given by $f_m=g^{|m|}$ [17], where g denotes the asymmetry parameter. The eigenvalues and the corresponding nontrivial solution of the system (8) can be obtained via an eigenvalue decomposition of the following symmetric tridiagonal matrix:

$$\mathbf{U}\boldsymbol{\Lambda}\mathbf{U}^{\mathrm{T}}=\begin{pmatrix}0&\beta_N&0&\cdots&\cdots&0&0\\ \beta_N&\ddots&\ddots&\ddots&\cdots&\cdots&0\\ 0&\ddots&0&\beta_1&0&\vdots&\vdots\\ \vdots&\ddots&\beta_1&0&\beta_1&\ddots&\vdots\\ \vdots&\vdots&0&\beta_1&0&\ddots&0\\ 0&\cdots&\cdots&\ddots&\ddots&\ddots&\beta_N\\ 0&0&\cdots&\cdots&0&\beta_N&0\end{pmatrix}, \tag{11}$$

where $\beta_m = 1/(2\sqrt{\sigma_{m-1}\sigma_m})$. Note that for the numerical implementation the Fourier series (4) must be truncated at $|n| \leqslant N$, where N is an odd number. The matrices $\mathbf{U}$ and $\mathbf{\Lambda}$ contain the orthogonal and normalized eigenvectors $|\nu\rangle$ with components $\langle m|\nu\rangle$ and the real-valued eigenvalues λ, respectively. Upon determination of the eigenvectors, the solution of (8) is obtained as $\langle m|u_n\rangle = \langle m|\nu\rangle/\sqrt{\sigma_m}$. It can be seen that this solution is independent of the discrete variable n and therefore the eigenvalue decomposition must be performed *once* only. In the appendix of our previous publication [15], readers can find analytical formulae regarding the eigenvector components of the tridiagonal matrix for avoiding a numerical iteration of these quantities. The general solution of the boundary-value problem is given by the superposition over all possible modes:

$$\psi_n(\rho,\varphi) = \sum_{\lambda_i>0} C_{in} \sum_{m=-N}^{N} (-1)^m \frac{\langle m|\nu_i\rangle}{\sqrt{\sigma_m}} I_{m-n}\left(\frac{\rho}{\lambda_i}\right) \mathrm{e}^{\mathrm{i}m\varphi}, \tag{12}$$

where the N unknown coefficients C_{in} must be found using the BC (6). This task can be accomplished as follows. Substituting the homogeneous solution (12) into (6), multiplying both sides with $\exp(-\mathrm{i}m'\varphi)$, integrating over the interval $\pi/2 \leqslant \varphi \leqslant 3\pi/2$ and using the integral relation

$$\int_{\pi/2}^{3\pi/2} \mathrm{e}^{\mathrm{i}m\varphi} \mathrm{e}^{-\mathrm{i}m'\varphi}\, \mathrm{d}\varphi = \pi(-1)^{m-m'} \operatorname{sinc}\left(\frac{m-m'}{2}\right), \tag{13}$$

where $\operatorname{sinc}(x) = \sin(\pi x)/(\pi x)$, yield a system of linear equations

$$\sum_{\lambda_i>0} C_{in} \sum_{m=-N}^{N} \frac{\langle m|\nu_i\rangle}{\sqrt{\sigma_m}} I_{m-n}\left(\frac{R}{\lambda_i}\right) \operatorname{sinc}\left(\frac{m-m'}{2}\right) = \frac{S_0}{2\pi^2} \exp[\mathrm{i}m'(\pi-\varphi_0)]. \tag{14}$$

For each value of the discrete variable n, taking equations for $|m'| = 0, 2, \ldots, N-1$, results in a well-conditioned system of N linearly independent equations for N unknown constants. After the determination of the constants, the obtained homogeneous solution must be inserted in series (4). The fluence within the circular bounded medium is obtained via integration as

$$\Phi(\boldsymbol{\rho}) = \int_0^{2\pi} \psi(\boldsymbol{\rho},\phi)\, \mathrm{d}\phi = \frac{2\pi}{\sqrt{\sigma_0}} \sum_{n=-N}^{N} \sum_{\lambda_i>0} C_{in} \langle 0|\nu_i\rangle I_n\left(\frac{\rho}{\lambda_i}\right) \exp(\mathrm{i}n\phi_{\boldsymbol{\rho}}). \tag{15}$$

For solving the above boundary-value, the source-free solution of the RTE must be finite for $\rho \to 0$. However, the complete solution of the homogeneous RTE contains additional modes of the form

$$\psi_n(\rho,\varphi) = \sum_{m=-\infty}^{\infty} \frac{\langle m|\nu_i\rangle}{\sqrt{\sigma_m}} K_{m-n}\left(\frac{\rho}{\lambda}\right) \mathrm{e}^{\mathrm{i}m\varphi}, \tag{16}$$

where $K_\nu(x)$ is the modified Bessel function of the second kind, which are needed for the solution of other boundary-value problems such as the circular ring and for defining the infinite space Green's function in terms of evanescent modes.

For the verification of the obtained homogenous solution in section 3, we additionally replaced the incident external source by an isotropic emitting δ-source inside the scattering medium. Therefore, the inhomogeneous BC (3) is replaced by the homogeneous BC:

$$\psi^{(h)}(\boldsymbol{\rho} \in \partial\mathcal{C}, \varphi) + \psi^{(p)}(\boldsymbol{\rho} \in \partial\mathcal{C}, \varphi) = 0, \qquad \pi/2 \leqslant \varphi \leqslant 3\pi/2, \tag{17}$$

where $\psi^{(h)}(\boldsymbol{\rho},\varphi)$ is the homogeneous solution with unknown constants and $\psi^{(p)}(\boldsymbol{\rho},\varphi)$ denotes the infinite space Green's function caused by the isotropic internal δ-source which can be obtained from our previous publication [15].

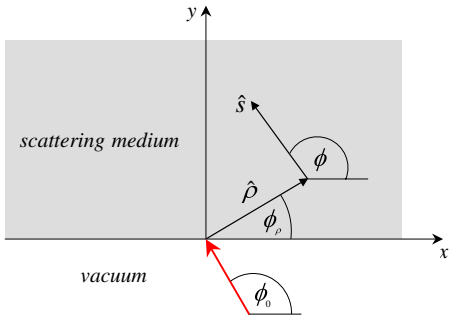

Figure 2. Semi-infinite medium with spatial and angular variables.

2.2. Radiative transfer in the semi-infinite geometry

The obtained solution for the circular bounded medium contains in principle the solution for the semi-infinite geometry if the radius of the circle is chosen very large. However, the evaluation of the above solution for large radii can lead to numerical instabilities caused by the enormous increase of the modified Bessel functions within the system of linear equations. Therefore, this section contains the solution of the two-dimensional RTE for the exact semi-infinite geometry. Similar to above, figure 2 shows schematically the geometry of the problem with all spatial and angular variables. The solution to the boundary-value problem in the semi-infinite geometry requires that the radiance must satisfy the inhomogeneous BC:

$$\psi(x, y = 0, \phi) = S_0 \delta(x)\delta(\phi - \phi_0), \qquad 0 \leqslant \phi < \pi. \tag{18}$$

Apart from the condition $\psi(\boldsymbol{\rho}, \phi) \to 0$ for $|x| \to \infty$, there are no additional BC regarding the spatial coordinate x. Therefore, the radiance is expanded by the Fourier integral

$$\psi(\boldsymbol{\rho}, \phi) = \frac{1}{2\pi} \int_{-\infty}^{\infty} \psi(\kappa, y, \phi)\, \mathrm{e}^{\mathrm{i}\kappa x}\, \mathrm{d}\kappa, \tag{19}$$

leading to a simplified version of (1) with only one spatial derivative

$$\left(\mu_t + \mathrm{i}\kappa \cos\phi + \sin\phi \frac{\partial}{\partial y}\right)\psi(\kappa, y, \phi) = \mu_s \int_0^{2\pi} f(\hat{\mathbf{s}} \cdot \hat{\mathbf{s}}')\psi(\kappa, y, \phi')\, \mathrm{d}\phi'. \tag{20}$$

The associated BC with (18) is

$$\psi(\kappa, y = 0, \phi) = S_0 \delta(\phi - \phi_0), \qquad 0 \leqslant \phi < \pi. \tag{21}$$

For solving the boundary-value problem in the semi-infinite geometry, we seek a solution in the form of the plane-wave mode

$$\psi(\kappa, y, \phi) = \mathrm{e}^{\xi y}\psi(\kappa, \phi), \tag{22}$$

where ξ and $\psi(\kappa, \phi)$ are the unknown eigenvalue and eigenfunction, respectively. Substituting this mode in the RTE (20) yields the eigenvalue problem

$$[\mu_t + k\cos(\phi - \phi_{\mathbf{k}})]\psi(\kappa, \phi) = \mu_s \int_0^{2\pi} f(\hat{\mathbf{s}} \cdot \hat{\mathbf{s}}')\psi(\kappa, \phi')\, \mathrm{d}\phi', \tag{23}$$

where $k = \sqrt{\mathbf{k} \cdot \mathbf{k}}$ and $\phi_{\mathbf{k}}$ denotes the direction of the complex wave vector

$$\mathbf{k} = \begin{pmatrix} \mathrm{i}\kappa \\ \xi \end{pmatrix} = k \begin{pmatrix} \cos\phi_{\mathbf{k}} \\ \sin\phi_{\mathbf{k}} \end{pmatrix}. \tag{24}$$

At this stage, all angular-dependent quantities of the RTE are expanded in the form of the modified Fourier series

$$\psi(\kappa, \phi) = \sum_{m=-\infty}^{\infty} (-1)^m \langle m|u\rangle \mathrm{e}^{\mathrm{i}m(\phi-\phi_{\mathbf{k}})}, \tag{25}$$

which depends explicitly on the direction of the wave vector **k** resulting in the recently introduced *method of rotated reference frames* (MRRF)[7–9]. Inserting the modified Fourier series (25) in the eigenvalue problem (23) results in the dispersion relation $k = \sqrt{\xi^2 - \kappa^2} = 1/\lambda$ which leads to the κ-dependent eigenvalues:

$$\xi = \xi(\kappa) = \pm\sqrt{\kappa^2 + \frac{1}{\lambda^2}}. \tag{26}$$

The unknown vector components are exactly the same as those for the circular geometry $\langle m|u\rangle = \langle m|v\rangle/\sqrt{\sigma_m}$. For the semi-infinite medium, the eigenvalues $\xi(\kappa)$ with positive sign can be excluded from the solution. Now, the direction of the wave vector follows from equation (24) as

$$\phi_{\mathbf{k}} = \arcsin\left(\frac{\xi}{k}\right) = -\frac{\pi}{2} + \mathrm{i}\,\mathrm{arsinh}(\lambda\kappa). \tag{27}$$

The general solution of the boundary-value problem for the semi-infinite geometry in the transformed space becomes the superposition

$$\psi(\kappa, y, \phi) = \sum_{\lambda_i>0} C_i(\kappa) \mathrm{e}^{\xi(\kappa)y} \sum_{m=-N}^{N} \frac{\langle m|v_i\rangle}{\sqrt{\sigma_m}} \exp\left[\mathrm{i}m\left(\phi - \frac{\pi}{2}\right)\right] \left[\lambda_i\kappa + \sqrt{1 + (\lambda_i\kappa)^2}\right]^m, \tag{28}$$

where the Fourier series has already been truncated for the numerical implementation. The procedure regarding the unknown constants is similar as for the circle, see above. Inserting the plane-wave modes in the BC (21), multiplying both sides with $\exp(-\mathrm{i}m'\phi)$ and integrating over the interval $0 \leqslant \phi \leqslant \pi$ result in the system of linear equations

$$\sum_{\lambda_i>0} C_i(\kappa) \sum_{m=-N}^{N} \frac{\langle m|v_i\rangle}{\sqrt{\sigma_m}} \mathrm{sinc}\left(\frac{m-m'}{2}\right) \left[\lambda_i\kappa + \sqrt{1 + (\lambda_i\kappa)^2}\right]^m = \frac{S_0}{\pi} \exp\left[\mathrm{i}m'\left(\frac{\pi}{2} - \phi_0\right)\right], \tag{29}$$

where N equations for the values $|m'| = 0, 2, \ldots, N-1$ have to be considered. Again, the fluence within the semi-infinite medium in the transformed space is given by the integration of the radiance and becomes the simple form

$$\Phi(\kappa, y) = \frac{2\pi}{\sqrt{\sigma_0}} \sum_{\lambda_i>0} C_i(\kappa) \langle 0|v_i\rangle \mathrm{e}^{-\sqrt{\kappa^2 + 1/\lambda_i^2}\,y}. \tag{30}$$

Note that the above method can be easily expanded for obtaining the solution in the slab geometry by considering additionally eigenvalues $\xi(\kappa)$ from equation (26) with a positive sign together with the resulting eigenfunctions.

3. Numerical results

In this section, the obtained solutions are validated against the Monte Carlo method, which we expect to converge in the limit of an infinitely large number of simulated photons to the exact solution of the RTE. For the following comparisons, the Henyey–Greenstein phase function with $g = 0.9$ is used. The optical properties of the scattering media are assumed to be $\mu_a = 0.01\,\mathrm{mm}^{-1}$ and $\mu_s = 10\,\mathrm{mm}^{-1}$ which are typically for biological tissue in the near-infrared spectral range.

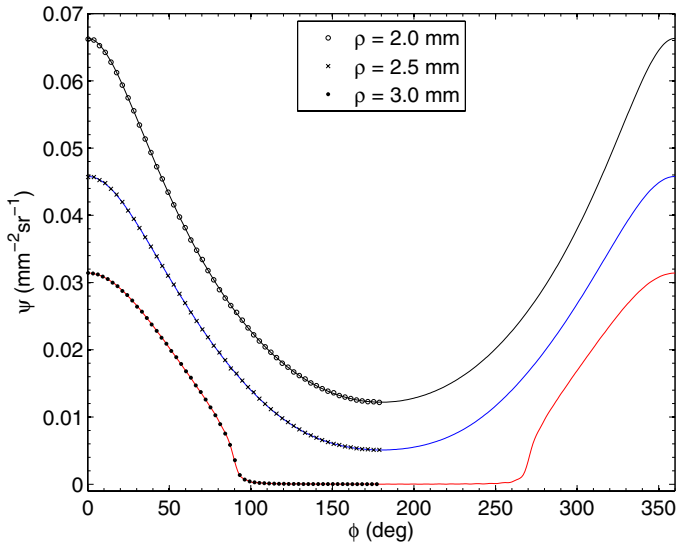

Figure 3. Angle-resolved Green's function caused by a isotropic δ-source which is located at the center of the circular bounded medium evaluated for three different distances. From the top to the bottom, the Fourier series are truncated at $N = 9$, $N = 7$ and $N = 21$.

3.1. Internal source in the circular bounded medium

For the first comparison, we consider an isotropic emitting δ-source $S(\boldsymbol{\rho}, \varphi) = \delta(\boldsymbol{\rho})/(2\pi)$ which is placed in the center of the circle with radius $R = 3\,\text{mm}$. In this case, the RTE is solved considering the homogeneous BC (17). The resulting radiance is evaluated for three different distances to the source and is shown in figure 3. The solid curves correspond to the analytical Green's function, whereas the symbols are the result of the Monte Carlo simulation. The influence of the implemented BC can be clearly seen. As intended, the radiance becomes zero at the circular boundary $\partial\mathcal{C}$ for all inward-pointing directions of the propagation vector $\hat{\mathbf{s}}$.

3.2. Oblique incident beam on the circular boundary

For the next comparison, an oblique incident beam having the direction $\varphi_0 = 160^\circ$ enters the circular bounded medium with radius $R = 5\,\text{mm}$ at the polar coordinates $(\rho, \phi_{\boldsymbol{\rho}}) = (R, 0)$. The resulting normalized radiance calculated at $\rho = 2\,\text{mm}$ with the analytical solution and the Monte Carlo method is shown in figure 4 for three different spatial angles $\phi_{\boldsymbol{\rho}}$. The radiance is normalized by the factor S_0.

The obtained analytical Green's function (solid curves) agrees in all simulations with the Monte Carlo method (noisy curves).

3.3. Perpendicular incident beam on the semi-infinite medium

In this comparison, it is assumed that a perpendicular incident beam enters the boundary of a semi-infinite medium. Figure 5 shows the resulting radiance normalized by S_0 and evaluated at $y = 2\,\text{mm}$ on the y-axis.

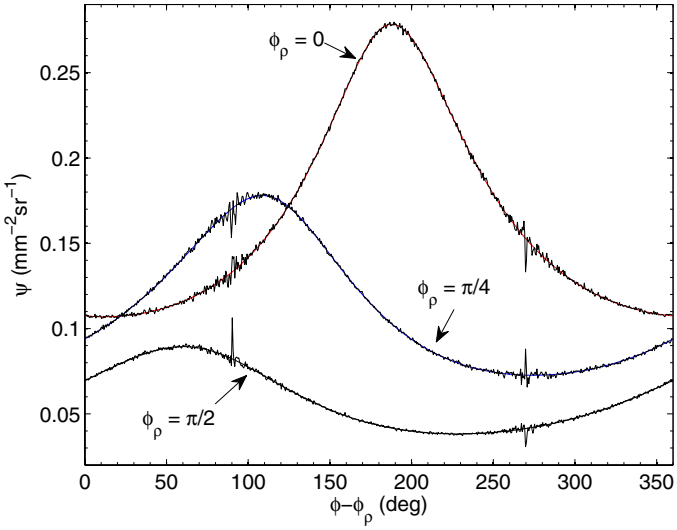

Figure 4. Angle-resolved Green's function caused by an oblique incident beam on the circular boundary evaluated for three different spatial positions. The Fourier series are truncated at $N = 15$.

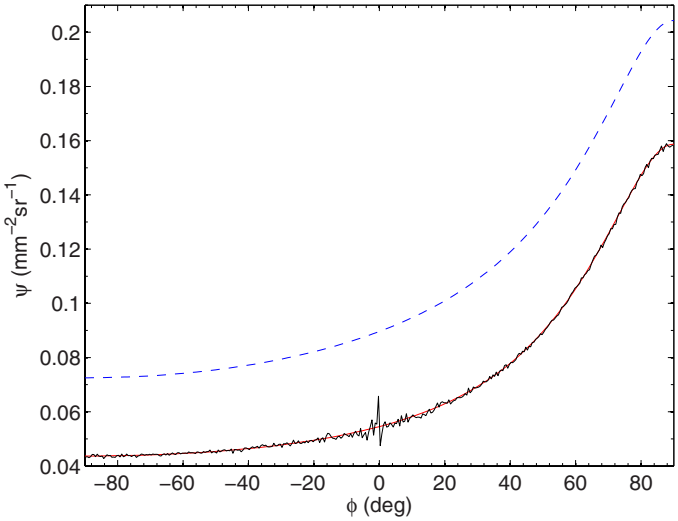

Figure 5. Angle-resolved Green's function caused by an perpendicular incident beam on the boundary of a semi-infinite medium evaluated at $y = 2$ mm on the y-axis. The Fourier series is truncated at $N = 13$.

As before, the analytical Green's function (solid curve) agrees well with the radiance obtained from the Monte Carlo method (noisy curve). In addition, the infinite space Green's function (dashed curve) is also shown to demonstrate the influence of the boundary.

4. Conclusions

In this study, the two-dimensional RTE is solved considering the exact boundary conditions for obtaining Green's functions in bounded anisotropically scattering media. Explicitly, the

circular and the semi-infinite geometry were considered. The numerical part of the resulting solutions is, apart from several constants which are obtained by solving systems of linear equations, the same as that for the infinite space Green's function. The derived solutions enable the consideration of an arbitrarily rotationally invariant phase function which must be expanded on the basis of complex exponentials. Within the derivations, no approximations are made, yielding excellent agreement compared to the Monte Carlo method. The relative differences between the analytical Green's function and the Monte Carlo simulations are only due to the finite number of simulated particles.

The derived formulae can be applied to obtain the solutions of simple two-dimensional radiative transfer problems, which are illuminated by external and/or internal sources. For example, an interesting application of the derived equations is the calculation of the spatially resolved reflectance and fluence of carbon fiber reinforced materials. Furthermore, it can be used for the verification of results obtained by numerical methods for solving the RTE.

Acknowledgment

We acknowledge the support by the European Union (nEUROPt, grant agreement no 201076).

References

[1] Case K M and Zweifel P F 1967 *Linear Transport Theory* (New York: Addison-Wesley)
[2] Duderstadt J J and Martin W R 1979 *Transport Theory* (New York: Wiley)
[3] Ishimaru A 1978 *Wave Propagation and Scattering in Random Media* (New York: Academic)
[4] Wang L, Jacques S L and Zheng L 1995 MCML—Monte Carlo modeling of light transport in multi-layered tissues *Comput. Methods Programs Biomed.* **47** 131–46
[5] Guo Z and Kumar S 2001 Discrete-ordinates solution of short-pulsed laser transport in two-dimensional turbid media *Appl. Opt.* **40** 3156–63
[6] Hielscher A H, Alcouffe R E and Barbour R L 1998 Comparison of finite-difference transport and diffusion calculations for photon migration in homogeneous and heterogeneous tissues *Phys. Med. Biol.* **43** 1285
[7] Markel V A 2004 Modified spherical harmonics method for solving the radiative transport equation *Waves Random Complex Media* **14** L13–9
[8] Panasyuk G, Schotland J C and Markel V A 2006 Radiative transport equation in rotated reference frames *J. Phys. A: Math. Gen.* **39** 115
[9] Machida M, Panasyuk G Y, Schotland J C and Markel V A 2010 The Green's function for the radiative transport equation in the slab geometry *J. Phys. A: Math. Theor.* **43** 065402
[10] Kim A 2004 Beam propagation in sharply peaked forward scattering media *J. Opt. Soc. Am.* A **21** 797–803
[11] Kim A 2004 Transport theory for light propagation in biological tissue *J. Opt. Soc. Am.* A **21** 820–7
[12] Klose A D, Netz U, Beuthan J and Hielscher A H 2002 Optical tomography using the time-independent equation of radiative transfer—part 1. Forward model *J. Quant. Spectrosc. Radiat. Transfer* **72** 691–713
[13] Barichello L B, Cabrera L C and Prolo Filho J F 2011 An analytical approach for a nodal scheme of two-dimensional neutron transport problems *Ann. Nucl. Energy* **38** 1310–7
[14] Ilyushin Y A and Budak V P 2011 Narrow-beam propagation in a two-dimensional scattering medium *J. Opt. Soc. Am.* A **28** 76–81
[15] Liemert A and Kienle A 2011 Radiative transfer in two-dimensional infinitely extended scattering media *J. Phys. A: Math. Theor.* **44** 505206
[16] Kienle A and Hibst R 2006 Light guiding in biological tissue due to scattering *Phys. Rev. Lett.* **97** 018104
[17] Heino J, Arridge S R, Sikora J and Somersalo E 2003 Anisotropic effects in highly scattering media *Phys. Rev.* E **68** 031908